Journal of Biomolecular NMR, **18:** 337–346, 2000.
KLUWER/ESCOM
© 2000 *Kluwer Academic Publishers. Printed in the Netherlands.*

HNCAN pulse sequences for sequential backbone resonance assignment across proline residues in perdeuterated proteins

Frank Löhr[a,*], Stefania Pfeiffer[a], Yi-Jan Lin[a], Judith Hartleib[a], Oliver Klimmek[b] & Heinz Rüterjans[a]

[a]*Institut für Biophysikalische Chemie and* [b]*Institut für Mikrobiologie, Johann Wolfgang Goethe-Universität Frankfurt am Main, Biozentrum N230, 1. OG, Marie Curie-Straße 9, D-60439 Frankfurt, Germany*

Received 7 July 2000; Accepted 21 September 2000

Key words: $^{2}H/^{13}C/^{15}N$-labelled proteins, proline, sequential assignment, slow $^{2}H/^{1}H$ exchange, triple-resonance NMR, TROSY

Abstract

A TROSY-based triple-resonance pulse scheme is described which correlates backbone ^{1}H and ^{15}N chemical shifts of an amino acid residue with the ^{15}N chemical shifts of both the sequentially preceding and following residues. The sequence employs $^{1}J_{NC\alpha}$ and $^{2}J_{NC\alpha}$ couplings in two sequential magnetization transfer steps in an 'out-and-back' manner. As a result, N,N connectivities are obtained irrespective of whether the neighbouring amide nitrogens are protonated or not, which makes the experiment suitable for the assignment of proline resonances. Two different three-dimensional variants of the pulse sequence are presented which differ in sensitivity and resolution to be achieved in one of the nitrogen dimensions. The new method is demonstrated with two uniformly $^{2}H/^{13}C/^{15}N$-labelled proteins in the 30-kDa range.

Introduction

Commonly used heteronuclear NMR experiments for backbone resonance assignment in $^{13}C/^{15}N$- or $^{2}H/^{13}C/^{15}N$-labelled proteins mostly rely on the detection of amide protons during acquisition (Bax and Grzesiek, 1993; Kay and Gardner, 1997). As a consequence, the 'sequential walk' along the main chain is interrupted at the positions of proline residues which lack nitrogen-bound protons. For doubly labelled proteins this problem can be circumvented by application of HACAN (Wang et al., 1995; Kanelis et al., 2000), CDCA(NCO)CAHA (Bottomley et al., 1999) or (HB)CBCA(CO)N(CA)HA (Kanelis et al., 2000) pulse sequences that finally detect C^{α}-bound protons and are able to provide correlations of proline resonances with those of adjacent residues. In a different approach, proline residues can be 'bridged' using the recently developed (H)CA(CO-TOCSY)NH and (H)CBCA(CO-TOCSY)NH experiments (Liu et al., 2000), which yield C^{α}-NH and C^{β}/C^{α}-NH connectivities between residues i and $i+2$, where $i+1$ can be a proline. A common feature of all these methods is the detection and/or excitation of carbon-bound protons, precluding their application to perdeuterated proteins which contain ^{1}H nuclei only at exchangeable sites.

Here we describe a novel experiment, termed HNCAN, which provides N,N-connectivities between a protonated amide group and amides of the preceding as well as the following residue. It is related to the HNCANNH pulse sequence (Weisemann et al., 1993; Ikegami et al., 1997) as it employs $^{1}J_{NC\alpha}$ and $^{2}J_{NC\alpha}$ couplings in two sequential magnetization transfer steps, but as a major difference, the HNCAN is of the 'out-and-back' rather than the 'out-and-stay' type. Hence, although the presence of an amide proton is mandatory for excitation at the start of the sequence and final detection, the amides of the two neighbouring residues may or may not be protonated. This enables sequential assignments across a proline

*To whom correspondence should be addressed. E-mail: murph@bpc.uni-frankfurt.de

residue, e.g. in position $i+1$, to be obtained by linking its ^{15}N chemical shift to those of residues i and $i+2$.

In ^{2}H/^{13}C/^{15}N labelled proteins that are expressed in D_2O and then transferred to H_2O solution, incomplete back exchange of strongly hydrogen-bonded amide protons may as well complicate assignment because the affected residues do not contain protons at all. Provided that the amides of the two adjacent residues are protonated, the gap in the chain of sequential connectivities can be closed in the same manner as indicated above for prolines.

Since one- and two-bond ^{15}N, $^{13}C^{\alpha}$ coupling constants in protein backbones are relatively small (Delaglio et al., 1991), long de- and rephasing periods of transverse ^{15}N and $^{13}C^{\alpha}$ magnetization are required to obtain the desired correlations. Nevertheless, an adequate sensitivity is achieved for the HNCAN experiment by taking advantage of the TROSY methodology (Pervushin et al., 1997; Salzmann et al., 1998) and high-level ^{2}H-labelling of protein samples to decelerate ^{15}N and $^{13}C^{\alpha}$ R_2 relaxation rates. In the following, two 3D HN(CA)N variants with slightly different coherence transfer pathways are presented.

Methods

The first pulse scheme for recording HN(CA)N spectra is depicted in Figure 1A. It is composed of standard pulse sequence elements described in the literature, and the mechanism of the individual coherence transfer steps shall not be repeated here in detail. Briefly, the magnetization transfer pathway can be summarized as

$$\mathrm{H}_i^{\mathrm{N}} \rightarrow \mathrm{N}_i \begin{array}{c}\nearrow\\ \searrow\end{array} \begin{array}{c}\mathrm{C}_i^{\alpha}\\ \\ \mathrm{C}_{i-1}^{\alpha}\end{array} \begin{array}{c}\nearrow\\ \searrow\\ \nearrow\\ \searrow\end{array} \begin{array}{cc}\mathrm{N}_{i+1} & (t_1)\\ \mathrm{N}_i & (t_1)\\ \mathrm{N}_{i-1} & (t_1)\end{array} \begin{array}{c}\searrow\\ \nearrow\\ \searrow\\ \nearrow\end{array} \begin{array}{c}\mathrm{C}_i^{\alpha}\\ \\ \mathrm{C}_{i-1}^{\alpha}\end{array}$$

$$\begin{array}{c}\searrow\\ \nearrow\end{array} \mathrm{N}_i(t_2) \rightarrow \mathrm{H}_i^{\mathrm{N}}(t_3). \qquad (1)$$

The experiment starts with polarizations of the amide proton and nitrogen of residue i, which is transferred in three successive INEPT (Morris and Freeman, 1979) steps to the amide nitrogens of residues $i-1$, i and $i+1$ using $^{1}J_{\mathrm{HN}}$, $^{1}J_{\mathrm{NC\alpha}}$ and $^{2}J_{\mathrm{NC\alpha}}$ scalar couplings. Following the t_1 evolution period, magnetization is transferred back to the amide proton via the reverse pathway. A TROSY (Pervushin et al., 1997) detection scheme is employed in order to take advantage of the partial cancellation of ^{1}H$^{\mathrm{N}}$-^{15}N dipole–dipole and ^{15}N or ^{1}H$^{\mathrm{N}}$ CSA relaxation contributions during periods where nitrogen and proton magnetization, respectively, resides in the transverse plane. It includes sensitivity enhancement (Cavanagh et al., 1991) combined with gradient echo/antiecho coherence selection (Kay et al., 1992) and the number of ^{1}H 180° pulses is minimized in the manner first described by Dingley and Grzesiek (1998). Application of the final 180° pulse on α-carbons concatenates the first τ' period of the TROSY scheme with the $^{13}C^{\alpha} \rightarrow {}^{15}N$ back transfer, slightly reducing the overall duration of the sequence (Loria et al., 1999; Salzmann et al., 1999a). Since only one component of the ^{1}H coupled ^{15}N doublet contributes to the finally observed signal, ^{15}N steady state magnetization can be exploited to enhance the sensitivity of the experiment by appropriate phase setting of the second ^{1}H 90° hard pulse (Pervushin et al., 1998).

The ^{15}N (t_1) evolution period is recorded under refocusing of $^{1}J_{\mathrm{NH}}$ interactions. Otherwise, while only the ^{15}N lowfield component of residue i would be detected owing to the TROSY selection at the end of the sequence, an undesired doublet splitting would occur for the cross peaks corresponding to residues $i-1$ and $i+1$. However, application of a pair of ^{1}H 180° pulses rather than a single one preserves the spin state of the $\mathrm{H}_i^{\mathrm{N}}$ amide proton in order to avoid the interchange of TROSY and anti-TROSY ^{15}N transitions between the Δ and T_N periods. Similarly, the water magnetization which is aligned along the positive z-axis after the initial INEPT sequence and, most importantly, before acquisition, using selective pulses and suitably adjusted phases of ^{1}H hard pulses (Grzesiek and Bax, 1993a; Stonehouse et al., 1994; Matsuo et al., 1996), is only temporarily inverted for a relatively short time $t_1/2$. This ensures minimal saturation of fast exchanging amide protons due to dephasing of water magnetization. A good suppression of residual transverse water magnetization is achieved using magic-angle gradients (Mattiello et al., 1996) such that the final ^{1}H 180° pulse could be applied non-selectively, deviating from the original implementations of the TROSY detection sequence employed here (Dingley and Grzesiek, 1998; Loria et al., 1999).

While nitrogen chemical shifts evolve as a function of t_2, the $^{13}C^{\alpha} \rightarrow {}^{15}N$ back transfer occurs simultaneously for a fixed duration $T_N + \tau'$, usually adjusted to the same value as Δ. To allow for t_2 acquisition times

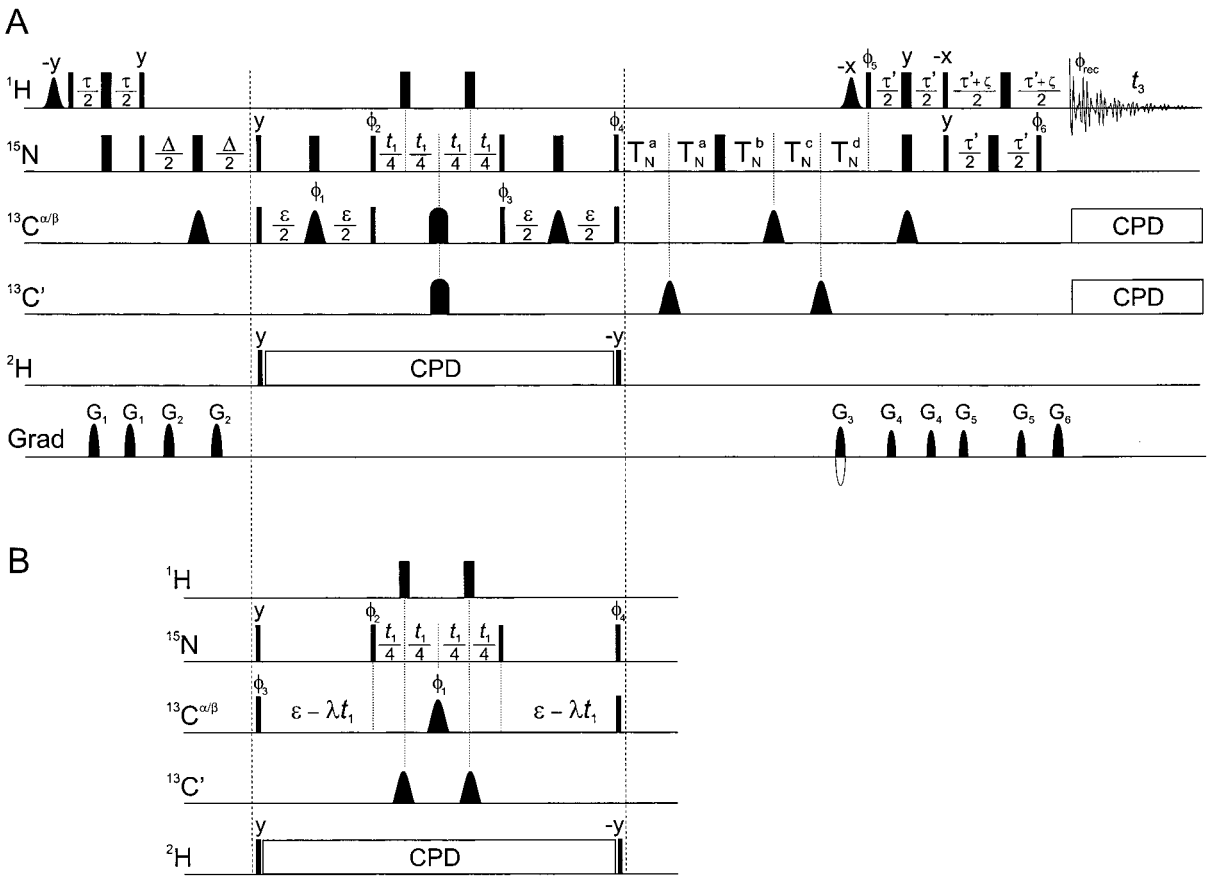

Figure 1. $^{13}C^{\alpha}$-^{15}N INEPT (A) and $^{13}C^{\alpha}$-^{15}N HMQC (B) variants of the HN(CA)N experiment. Only the central part of pulse sequence B is shown which replaces the corresponding section of A, as indicated by the dashed lines. Narrow and wide rectangles denote 90° and 180° pulses, respectively. Carrier offsets are 4.75 ppm (water) (^{1}H), 118.1 ppm (^{15}N), 56.0 ppm (^{13}C) and 4.7 ppm (^{2}H). The nitrogen carrier is temporarily shifted to 123.0 ppm after the second ^{15}N 90° pulse (applied with phase y) and is returned to its original position before the 90° pulse with the phase ϕ_4. Pulse widths indicated in the following are suitable for a B_0 field corresponding to 800 MHz ^{1}H frequency. Selective water-flip-back pulses have a Gaussian shape, truncated at 10%, and a duration of 3 ms. The width of rectangular 90° $^{13}C^{\alpha}$ pulses is adjusted to 39.5 μs, causing minimal excitation in the carbonyl region (Kay et al., 1990). 180° pulses on α-carbons, applied during periods Δ and T_N, are 300 μs G^3 Gaussian cascades (Emsley and Bodenhausen, 1990). The $^{13}C^{\alpha/\beta}$ G^3 pulses at the centre of the ε periods have durations of 220 μs and are applied at an offset corresponding to 43.6 ppm using phase modulation (Patt, 1992). In sequence A, refocusing of ^{15}N, $^{13}C^{\alpha}$ and ^{15}N, $^{13}C'$ couplings during t_1 is accomplished by a single 500-μs ^{13}C WURST-20 (Kupçe and Freeman, 1995) pulse (80 kHz sweep) centered at 106 ppm, while in sequence B two carbonyl-selective pulses are applied during t_1 to avoid an evolution of ^{15}N, $^{13}C'$ and $^{13}C'$, $^{13}C^{\alpha}$ couplings. Carbon decoupling during acquisition is implemented as a sequence of 3-ms WURST pulses, employing a five-step supercycle (Tycko et al., 1985). Phase modulated carbonyl 180° pulses, applied at a frequency corresponding to 176 ppm, have the shape of the centre lobe of a sinc function and a width of 100 μs. Deuterium decoupling is achieved with a WALTZ-16 sequence (Shaka et al., 1983) applied along the x-axis with an RF field strength of 0.9 kHz. Fixed delays are adjusted as follows: $\tau = 4.6$ ms, $\Delta = 22$–28 ms, ε (sequence A) $= 28$ ms, ε (sequence B) $= 40$ ms, $\tau' = 5.4$ ms, $\zeta = 0.6$ ms. In order to manipulate the signal decay due to modulations with scalar couplings in the t_1 dimension of sequence B, the factor λ can be varied between 0 and 0.5 (see text for explanation). Evolution of ^{15}N chemical shifts is implemented in a semi-constant time manner where $T_N^a = (\Delta - \tau' - \chi\, t_2)/4$; $T_N^b = [(1 - \chi)\, t_2)]/2$; $T_N^c = (\Delta - \tau' + \chi\, t_2)/4$; $T_N^d = (\Delta - \tau' + (2 - \chi)\, t_2)/4$, and the factor χ is given by $\Delta - \tau'$ divided by the desired ^{15}N acquisition time if longer than $\Delta - \tau'$, otherwise $\chi = 1$. The default pulse phase is x. Phases are cycled according to: ϕ_1 =x, y, −x, −y; $\phi_2 = 2$(x), 2(−x); $\phi_3 = 4$(x), 4(−x); $\phi_4 = 8$(y); 8(−y); ϕ_5 = y, ϕ_6 = x; ϕ_{rec} = R, 2(−R), R, where R = x, 2(−x), x. Quadrature detection in t_1 is achieved by altering ϕ_2 in the States-TPPI (Marion et al., 1989) manner. All gradients are sine-bell shaped and have the following durations, approximate strengths at their center and directions: G_1, 1.0 ms, 5 G/cm, x; G_2, 1.0 ms, 7.5 G/cm, y; G_3, 0.8 ms, 39.45 G/cm, xyz; G_4, 0.5 ms, 4 G/cm, x; G_5, 0.5 ms, 5.5 G/cm, y; G_6, 0.4 ms, 8 G/cm, xyz. N- and P-type coherences are collected alternately by inverting the polarity of G_3 along with pulse phases ϕ_5 and ϕ_6. Axial peaks are shifted to the edge of the spectrum by incrementing ϕ_4 and the receiver phase by 180° for each value of t_2. The phase of the second rectangular 90° pulse on protons is adjusted for a Bruker Avance spectrometer to constructively add components originating from ^{1}H and ^{15}N steady-state magnetizations. On other spectrometer types phase inversion of the latter pulse together with the initial selective 90° pulse may be required.

longer than T_N ($\equiv 2T_N^a + T_N^b + T_N^c + T_N^d$ at $t_2 = 0$), the evolution period is of the semi-constant time (Logan et al., 1992; Grzesiek and Bax, 1993b) type (see figure legend for details). Carbon decoupling during acquisition is optional but it is recommended, as it results in a slightly enhanced sensitivity and purely absorptive lineshapes (Yang and Kay, 1999). For application to $^2H/^{13}C/^{15}N$-labelled proteins, ^2H decoupling during the ε delays is mandatory in order to eliminate the effect of the large deuterium quadrupolar interaction (Grzesiek et al., 1993), which would otherwise cause a relatively fast decay of $^{13}C^\alpha$ coherences. The decoupling is not interrupted during t_1, as it also results in line-narrowing of ^{15}N resonances in residues where the initially deuterated amides did not exchange with H_2O.

The 3D HN(CA)N experiment yields ω_1/ω_2 diagonal peaks and cross peaks at resonance positions $^{15}N_i$, $^{15}N_{i-1}$ and $^{15}N_{i+1}$ along the ω_1 axis with signal amplitudes proportional to

$$[\sin^2(\pi\,{}^1J_{NC\alpha}\Delta)\cos^2(\pi\,{}^2J_{NC\alpha}\Delta) + \cos^2(\pi\,{}^1J_{NC\alpha}\Delta)\sin^2(\pi\,{}^2J_{NC\alpha}\Delta)] \times \cos^2(\pi\,{}^1J_{NC\alpha}\varepsilon)\cos^2(\pi\,{}^2J_{NC\alpha}\varepsilon)\cos^2(\pi\,{}^1J_{C\alpha C\beta}\varepsilon)\cos(\Omega_{Ni}t_1) \quad (2a)$$

$$\cos^2(\pi\,{}^1J_{NC\alpha}\Delta)\sin^2(\pi\,{}^2J_{NC\alpha}\Delta)\sin^2(\pi\,{}^1J_{NC\alpha}\varepsilon)\sin^2(\pi\,{}^2J_{NC\alpha}\varepsilon)\cos^2(\pi\,{}^1J_{C\alpha C\beta}\varepsilon)\cos(\Omega_{Ni-1}t_1) \quad (2b)$$

$$\sin^2(\pi\,{}^1J_{NC\alpha}\Delta)\cos^2(\pi\,{}^2J_{NC\alpha}\Delta)\sin^2(\pi^1J_{NC\alpha}\varepsilon)\sin^2(\pi\,{}^2J_{NC\alpha}\varepsilon)\cos^2(\pi\,{}^1J_{C\alpha C\beta}\varepsilon)\cos(\Omega_{Ni+1}t_1), \quad (2c)$$

ignoring relaxation effects and for simplicity assuming that $^1J(N_i, C_i^\alpha) = {}^1J(N_{i-1}, C_{i-1}^\alpha)$ and $^2J(N_i, C_{i-1}^\alpha) = {}^2J(N_{i+1}, C_i^\alpha)$ and that $T_N + \tau'$ is adjusted to Δ. It is apparent that the relative intensity of diagonal and cross peaks critically depends on the ε delay. In order to remove the effect of passive $^1J_{C\alpha C\beta}$ couplings ε should be set to $n/^1J_{C\alpha C\beta}$. For average coupling constants $^1J_{NC\alpha} = 10.5$ Hz, $^2J_{NC\alpha} = 7.5$ Hz (Delaglio et al., 1991), $^1J_{C\alpha C\beta} = 35$ Hz and with $\Delta = T_N + \tau' = 24$ ms, $\varepsilon = 28$ ms (i.e. $n = 1$), $t_1 = 0$ the factors 2a–c amount to 0.114, 0.034 and 0.086 for $^{15}N_i$, $^{15}N_{i-1}$ and $^{15}N_{i+1}$ resonances, respectively.

Cross peak intensities might be considerably increased relative to diagonal peaks by using longer ε periods. However, with $n = 2$ the total time 2ε during which transverse relaxation of $^{13}C^\alpha$ magnetization takes place would be longer than 100 ms, leading to an unacceptable sensitivity loss for most proteins even if perdeuteration is employed. As a compromise, the sum of $^{13}C^\alpha$-^{15}N de- and rephasing periods, 2ε, can be adjusted to $3/^1J_{C\alpha C\beta}$ (≈80 ms) if the two central INEPT transfer steps are replaced by a $^{13}C^\alpha$-^{15}N HMQC module. The required modification of the 3D HN(CA)N pulse sequence is outlined in Figure 1B. In this variant the factor $\cos(\pi^1J_{C\alpha C\beta}\ 2\varepsilon)$ substitutes for $\cos^2(\pi^1J_{C\alpha C\beta}\varepsilon)$ in expressions 2a–c. Assuming the same coupling constants as above, relative signal intensities of $^{15}N_i$, $^{15}N_{i-1}$ and $^{15}N_{i+1}$ resonances are 0.009, 0.070 and 0.179, respectively, for $\varepsilon = 40$ ms. Thus, while diagonal peaks which yield redundant chemical shift information are virtually completely suppressed, the transfer efficiencies for cross peaks are enhanced more than twofold. On the other hand, $^{13}C^\alpha$ relaxation proceeds for a further 24 ms compared to the $^{13}C^\alpha$-^{15}N INEPT variant of Figure 1A, resulting in a non-negligible attenuation of diagonal and cross peaks. It should be noted that due to the factor $\cos(\pi^1J_{C\alpha C\beta}\ 2\varepsilon)$, $i-1$ and $i+1$ cross peak intensities are inverted if a glycine residue is in position $i-1$ or i, respectively, which may provide valuable information for sequence specific assignments.

A drawback of the $^{13}C^\alpha$-^{15}N HMQC-type correlation is that a modulation with the passive $^1J_{C\alpha C\beta}$ coupling is imposed on the t_1 period, limiting the resolution in the first ^{15}N domain. The impact of the latter scalar interaction can be alleviated by simultaneously incrementing the time for ^{15}N chemical shift evolution while decrementing the ε delay as a function of t_1. As a consequence, line-broadening due to $^1J_{C\alpha C\beta}$ and $^{13}C^\alpha$ transverse relaxation is scaled down at the expense of modulations with the smaller $^1J_{NC\alpha}$ and $^2J_{NC\alpha}$ couplings. Thus the t_1 interferogram is enveloped by

$$\cos[\pi^1J_{C\alpha C\beta}(2\varepsilon + (1-2\lambda)t_1))] \sin^2[\pi^1J_{NC\alpha}(\varepsilon - \lambda t_1)]\sin^2[\pi^2J_{NC\alpha}(\varepsilon - \lambda t_1)] \times \exp(-t_1/T_{2,N})\exp[-(1-2\lambda)t_1/T_{2,C\alpha})]. \quad (3)$$

Expression 3 is valid for cross peaks, whereas for (usually unobservable) diagonal peaks the sine terms would have to be replaced by cosine terms with identical arguments. A graphical representation of Equation 3, illustrating the dependence on the scaling factor λ, is presented in Figure 2. With $\lambda = 0.25$ a relatively flat curve is obtained, approximating a constant-time evolution period for $t_1(\max) \lessapprox 15$ ms, whereas with $\lambda = 0$ (i.e. a conventional evolution period) or $\lambda = 0.5$ (constant duration of $^{13}C^\alpha$ transverse magnetization) a more pronounced signal decay occurs during t_1, precluding long acquisition times. The initial ascent of the curves for $\lambda < 0.5$ arises because 2ε is slightly shorter than $3/^1J_{C\alpha C\beta}$.

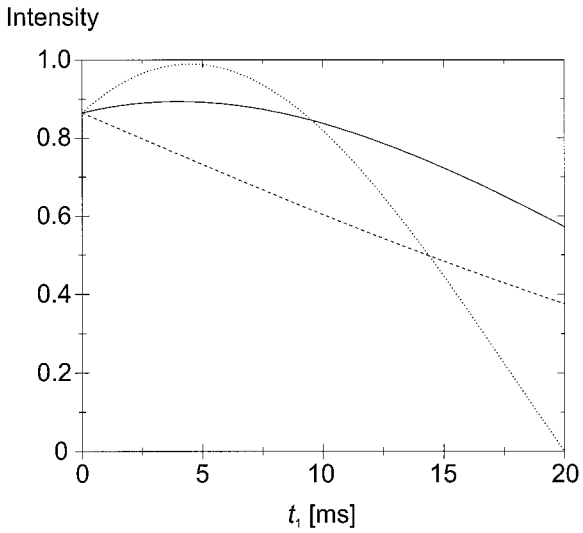

Figure 2. Modulation of cross peak intensities with the t_1 evolution time in the pulse sequence of Figure 1B using scaling factors $\lambda = 0$ (dotted line), $\lambda = 0.25$ (solid line) and $\lambda = 0.5$ (dashed line) according to expression (3). The delay ε was adjusted to 40 ms and the following coupling constants were assumed: $^1J_{C\alpha C\beta} = 35$ Hz, $^1J_{NC\alpha} = 10.5$ Hz, $^2J_{NC\alpha} = 7.5$ Hz. Transverse relaxation times were estimated to be 100 ms for $^{13}C^{\alpha}$ and 200 ms for the slowly relaxing ^{15}N TROSY component in a perdeuterated protein. The vertical scale is given in arbitrary units.

Experimental

NMR samples

Pulse sequences have been applied to two uniformly $^2H/^{13}C/^{15}N$-labelled proteins, the dimeric polysulfide-sulfur transferase (formerly sulfide dehydrogenase, Sud) from *Wolinella succinogenes* (Kreis-Kleinschmidt et al., 1995) and the monomeric diisopropylfluorophosphatase (DFPase) from *Loligo vulgaris*. Both proteins were expressed in *E. coli* grown on $^2H/^{13}C/^{15}N$-enriched media based on algal lysates. The Sud protein including a His-tag (Sud-His_6) was dissolved in 50 mM potassium phosphate buffer (95% H_2O/5% D_2O, pH = 7.6), containing 14 mM Na_2S and 1 mM $Na_2S_4O_6$ to yield a (dimer) concentration of 0.6 mM. Under these solvent conditions 1 mM polysulfide [S] is formed, resulting in a covalently attached chain of up to 10 polysulfide-sulfur atoms at the single cysteine residue of each monomer of the Sud dimer (Klimmek et al., 1999). The concentration of DFPase was 0.9 mM in 10 mM Bis-Tris-propane (1,3-bis[tris-(hydroxymethyl)-methylamino]-propane) buffer (95% H_2O/5% D_2O) at pH = 6.3. Sample volumes were 300 µl contained in Shigemi microcells.

Data acquisition and processing

Spectra were recorded at ^1H Larmor frequencies of 800.13 or 600.13 MHz using four-channel Bruker Avance spectrometers equipped with 5 mm $^1H/^{13}C/^{15}N$ xyz-gradient triple resonance probes. Temperature settings were 26 °C or 28 °C for experiments on Sud and DFPase samples, respectively.

In the HN(CA)N experiment (recorded at 800 MHz using the pulse sequence of Figure 1A) on Sud, the Δ ($=T_N + \tau'$) period had a duration of 24 ms and spectral widths comprised 39.5 ppm (^{15}N, ω_1), 25.7 ppm (^{15}N, ω_2) and 11.2 ppm (^1H, ω_3). Time domain data consisted of 58 × 48 × 768 complex points, corresponding to acquisition times of 18.1, 23.0 and 85.4 ms in t_1, t_2 and t_3, respectively, such that the factor χ of the semi-constant time t_2 period was adjusted to 0.8. Sixteen scans were accumulated per FID, resulting in a measuring time of 3.7 days.

The $^{13}C^{\alpha}$-^{15}N HMQC version of the HN(CA)N was applied to the DFPase sample at 800 MHz using $\Delta = T_N + \tau' = 26$ ms and $\chi = 0.9$. The factor λ of Figure 1B was adjusted to 0.25. Spectral widths comprised 42.6 ppm (^{15}N, ω_1), 29.4 ppm (^{15}N, ω_2) and 13.4 ppm (^1H, ω_3) and acquisition times (number of complex points) were 15.1 ms (52) in t_1, 23.5 ms (56) in t_2 and 95.9 ms (1024) in t_3. Data acquisition required 4.8 days of measuring time, using 16 scans per FID.

For a quantitative comparison, both the $^{13}C^{\alpha}$-^{15}N INEPT and $^{13}C^{\alpha}$-^{15}N HMQC versions were applied to DFPase at 600 MHz employing identical acquisition parameters. Delays $\Delta = T_N + \tau'$ were set to 24 ms and the factor χ was adjusted to 0.73. Spectral widths were

37.0, 29.4 and 11.0 ppm in the ^{15}N (ω_1), ^{15}N (ω_2) and ^{1}H (ω_3) domains, respectively. Acquisition times were 16.0 (t_1), 26.9 (t_2) and 77.5 ms (t_3), corresponding to $36 \times 48 \times 512$ complex data points. Accumulation of 16 scans per FID gave rise to measuring times of 72 h for each experiment.

Processing of Sud and DFPase spectra was carried out using the XWIN-NMR (Bruker) and NMRPipe/NMRDraw (Delaglio et al., 1995) programs, respectively. Linear prediction was applied in indirectly detected dimensions of all spectra to extend time domain data. In the first ^{15}N dimension of all spectra acquisition was delayed by two dwell-times due to the presence of relatively long ^{13}C refocusing pulses. In order to avoid first order phase corrections, the missing first points were constructed by linear prediction. Prior to Fourier transformation and zero-filling, data were apodized with squared-cosine weighting functions in all dimensions. After discarding the high-field halves of the spectra in the proton dimension, matrices consisted of $256 \times 128 \times 1024$ (Sud), $256 \times 256 \times 1024$ (DFPase, 800 MHz) or $128 \times 128 \times 512$ (DFPase, 600 MHz) real data points.

Results and discussion

The utility of the HNCAN experiment was tested with two proteins in the 30-kDa range for which resonance assignments currently are in progress in our laboratory and will be reported elsewhere. Polysulfide-sulfur transferase (Sud-His_6) is a dimeric protein consisting of two identical subunits of 137 amino acid residues (MW 30.6 kDa). Each monomer contains 8 proline residues, for all of which sequence specific ^{15}N resonance assignments could be obtained with the HN(CA)N method. Figure 3 shows ω_1/ω_3 strips taken from the 3D spectrum recorded with the $^{13}C^{\alpha}$-^{15}N INEPT-type pulse sequence of Figure 1A, demonstrating the assignment of prolines 27, 81, 84 and 126. As an example, the nitrogen of P27 is involved in N,N correlations with both the preceding and following amino acid. Thus, residues S26 and K28 are unambiguously linked via $i + 1$ and $i - 1$ connectivities, respectively, to a common ^{15}N chemical shift, although no correlations are available for the residue inbetween due to the missing amide proton. For perdeuterated proteins, similar information cannot be obtained by any other experiment published so far.

The HN(CA)N experiment was particularly useful during assignment of residues E82 and K83 of Sud, also shown in Figure 3. Using [^{15}N,^{1}H]-TROSY versions (Salzmann et al., 1999b) of established H^N-detected triple-resonance experiments like HNCACB (Wittekind and Mueller, 1993) and HN(CA)CO (Clubb et al., 1992), it became obvious that they were sequential neighbours, but it was not a priori clear why no further sequential connectivities via common $^{13}C^{\alpha}$, $^{13}C^{\beta}$ and $^{13}C'$ chemical shifts could be identified on either side. Inspection of the 3D HN(CA)N spectrum, however, revealed that these residues were enclosed by two prolines, which immediately enabled their sequence specific assignment. In some instances (e.g. K83, G124, L125) only $i + 1$ but no $i - 1$ cross peaks were detectable due to sensitivity reasons, but nevertheless the HN(CA)N yielded valuable information either supporting or negating tentative assignments resulting from the above mentioned spectra.

The second protein, diisopropylfluorophosphatase (DFPase), contains 314 amino acid residues (MW 35.1 kDa), 20 of which are prolines. Approximately one third of the backbone amides of non-proline residues exhibit very slow exchange with the solvent. As a consequence, in ^{2}H/^{13}C/^{15}N-labelled samples these amides do not back-exchange upon transfering the protein into H_2O solution and remain unobservable in ^{1}H detected experiments after a period as long as one year, whereas in ^{1}H-^{15}N correlation spectra of non-deuterated samples the expected number of signals is readily detected. The high portion of non-protonated amides seriously interferes with the sequential backbone assignment as based on established triple-resonance methods, most of which require a perdeutered sample of DFPase because of otherwise unfavourable relaxation properties associated with its relatively high molecular weight. As demonstrated in the following, the HN(CA)N experiment reduces these difficulties to a considerable extent.

Figure 4A illustrates the sequential assignment of a fragment of 11 residues near the N-terminus of DFPase which includes two prolines, P4 and P8. Since the $^{13}C^{\alpha}$-^{15}N HMQC version of the HN(CA)N pulse sequence was employed here, the spectrum is free from diagonal peaks and each ω_1/ω_3 strip contains one cross peak at the ^{15}N chemical shift of the following residue and a second, usually weaker, at the ^{15}N chemical shift of the preceding residue. These chemical shifts correspond to the ω_2 position of the plane which contains the cross peak pair of the adjacent amino acid, unless it is a proline. In the latter case the second neighbour of the proline is identified by the

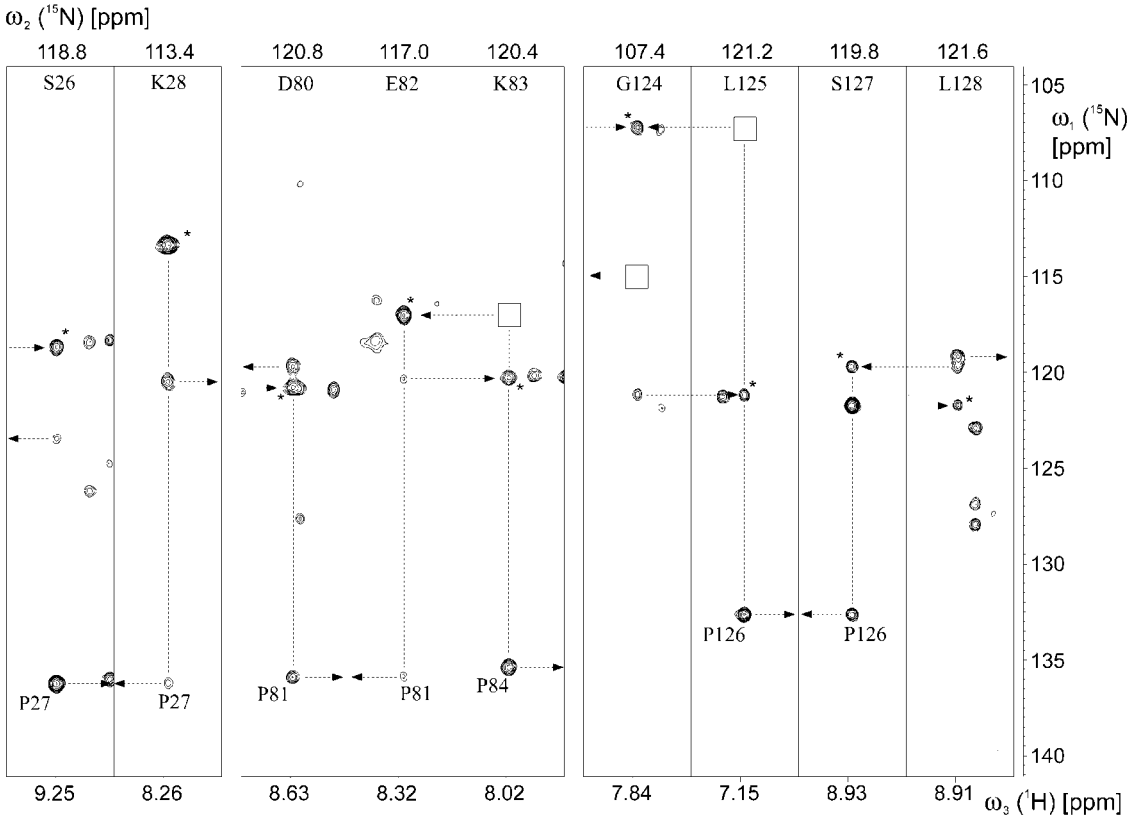

Figure 3. Sections of ω_1/ω_3 slices from a HN(CA)N spectrum ($^{13}C^{\alpha}$-^{15}N INEPT version of Figure 1A) of Sud taken through the ^{15}N chemical shifts of the residues given at the top of each panel. Along ω_3, strips are centered around the corresponding amide proton chemical shifts and have a width of 0.3 ppm. ^{15}N (ω_1/ω_2) diagonal peaks are labelled with asterisks. Empty boxes indicate the position of expected but undetected $i-1$ cross peaks. The vertical dashed lines connect diagonal and cross peaks belonging to the considered residue while horizontal arrows connect $i-1$ or $i+1$ cross peaks with the diagonal peaks of the sequential neighbour. For prolines, only cross peaks are obtained along ω_1 at the $^{15}N/^{1}H$ (ω_2/ω_3) chemical shifts of the two adjacent residues. Contours are drawn on an exponential scale using a factor of $2^{1/2}$.

coincidence of cross peak positions along ω_1 in the characteristic region downfield from $\approx$ 132 ppm such that the 'sequential walk' along the protein backbone can be continued.

The backbone ^{15}N assignment in the presence of deuterated amides is demonstrated in Figure 4B. In the $^{2}H/^{13}C/^{15}N$-labelled sample of DFPase, I165 and V167 are among those residues whose amide hydrogens did not noticeably exchange with the solvent after expression of the protein in D_2O. Their ^{15}N resonances could however be assigned via N,N-connectivities to adjacent amino acids in the 3D HN(CA)N spectrum. In each case the assignments were confirmed by correlations between the observed ^{15}N chemical shift and the $^{13}C'$ chemical shifts of the respective preceding residue in a [^{15}N,^{1}H]-TROSY-HNCO (Ikura et al., 1990; Salzmann et al., 1998) spectrum recorded on ^{13}C,^{15}N-labelled DFPase, taking into account a downfield shift of approximately 0.8 ppm due to the absence of deuterium isotope effects on ^{15}N in the latter sample, whereas these cross peaks were missing in the HNCO spectrum of the deuterated protein. It should be mentioned that an assignment strategy based on triple-resonance spectra of non-deuterated protein, which would not suffer from slow-exchanging amides, proved to be unsuccessful because of insufficient sensitivity of crucial experiments such as HNCACB and HN(CA)CO.

Residue Q166 of DFPase (Figure 4B) is isolated in a sense that the amide nitrogens of both the preceding and following amino acid are deuterated. Consequently, its assignment in any other triple-resonance experiment recorded on the ^{2}H,^{13}C,^{15}N-labelled sample is impossible, whereas it is straightforward with the help of the HN(CA)N. However, its utility for the sequential assignment across non-protonated amides

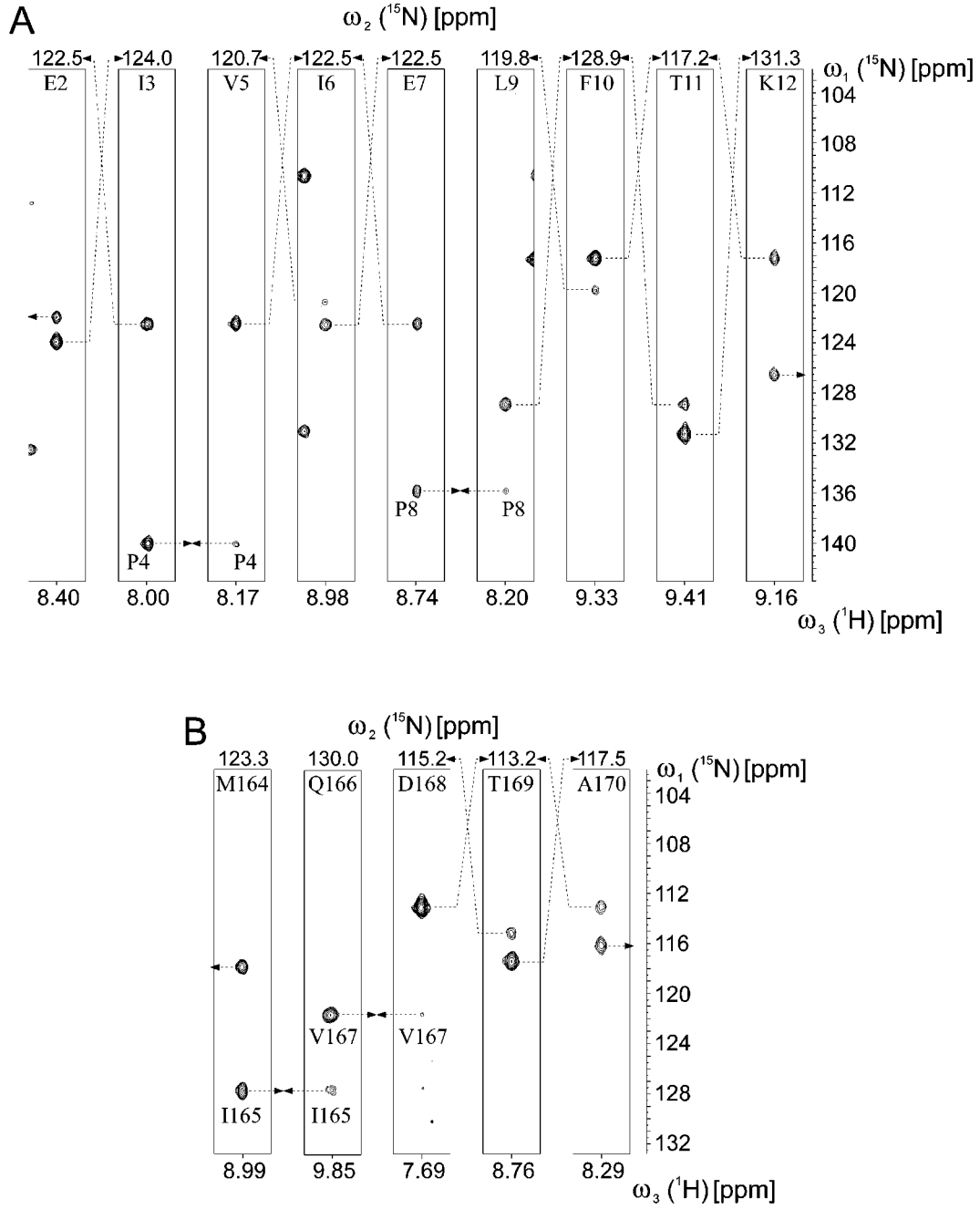

Figure 4. Application of the $^{13}C^{\alpha}$-^{15}N HMQC version of the HN(CA)N (recorded at 800 MHz) for the sequential assignment of residues E2 to K12 (A) and M164 to A170 (B) of DFPase. The strips with a width of 0.16 ppm are taken at the ^{15}N (ω_2) positions and centered at the $^1H^N$ (ω_3) positions of the residues given at the top of each panel. Sequential connectivities are obtained by simultaneously matching the ^{15}N (ω_1) chemical shift of one cross peak with the ^{15}N (ω_2) chemical shift of another and vice versa, as indicated by broken arrows. Cross peaks involving ^{15}N resonances of prolines and of deuterated amides are labelled with the corresponding residue number. Here, the two neighbouring residues are identified by common ^{15}N chemical shifts along ω_1. Only positive contour levels, spaced by a factor of $2^{1/2}$, are drawn.

is limited to cases where the backbone nitrogens of both flanking residues are protonated. This contrasts methods such as HACAN, CDCA(NCO)CAHA or (HB)CBCA(CO)N(CA)HA which even provide sequential assignments for poly-proline stretches in non-deuterated protein samples. Application of the HN(CA)N experiment yielded sequence specific ^{15}N resonance assignments for 16 prolines of DFPase, whereas for the remaining 4 this could not be achieved because the amide nitrogens at both sides were either deuterated or yet unassigned.

In order to assess the relative sensitivities of the $^{13}C^{\alpha}$-^{15}N INEPT- and $^{13}C^{\alpha}$-^{15}N HMQC-type pulse sequences, both versions were also recorded at 600 MHz using the same sample (DFPase) and identical experimental conditions. Evaluation of the intensities of 168 cross peaks that are well resolved in both spectra yielded $I_{\mathrm{HMQC}}/I_{\mathrm{INEPT}}$ ratios covering a relatively wide range of 0.6 to 2.3, which reflects variations in the $^{13}C^{\alpha}$ R_2 relaxation rates as well as in $^1J_{\mathrm{NC}\alpha}$ and $^2J_{\mathrm{NC}\alpha}$ coupling constants. The average signal enhancement was 1.2 in favor of the $^{13}C^{\alpha}$-^{15}N HMQC version. For larger proteins, exhibiting faster transverse relaxation of $^{13}C^{\alpha}$ magnetization, however, the $^{13}C^{\alpha}$-^{15}N INEPT variant might be superior.

Inherent to the $^{13}C^{\alpha}$-^{15}N HMQC variant recorded with $2\varepsilon \approx 3/^1J_{\mathrm{C}\alpha\mathrm{C}\beta}$ is the suppression of diagonal peaks, reducing the chance of overlap in the ω_1 dimension. On the other hand, the redundant information provided by diagonal peaks in the INEPT-type sequence is useful in the actual sequential connection of peaks, avoiding additional uncertainty during matching of ^{15}N frequencies in different dimensions. An obvious way to improve the resolution is the introduction of a fourth dimension which disperses overlapping cross peaks along a $^{13}C^{\alpha}$ axis. This can easily be achieved for either type of the HNCAN pulse scheme, replacing fixed ε periods by constant-time evolution periods. Such a 4D experiment has been successfully carried out on the DFPase sample and provided unambiguous connectivities even where $^{15}N_{i+1}$ and $^{15}N_{i-1}$ resonances adjacent to a given residue are degenerate (results not shown). However, the additional measurement time requirement of almost six days appears not to be justified in many cases.

Conclusions

We have introduced HNCAN pulse sequences to provide sequence-specific ^{15}N chemical shifts of proline residues in ^{2}H/^{13}C/^{15}N-labelled proteins, a piece of information which, to our knowledge, is unavailable from any other method published so far. Since nitrogen resonances are correlated with those of both the preceding and following amino acid, backbone connectivities across prolines can be detected, provided that the two adjacent residues are not prolines, too. The new method is not limited to the assignment of prolines but rather complements the established $^1H^N$-based assignment strategy relying on intra- and inter-residual correlations to common ^{13}C chemical shifts and may remove ambiguities thereof. In favourable cases, problems due to a failure to detect amide protons because of either fast ^{1}H/^{1}H or very slow ^{2}H/^{1}H exchange with the solvent, as sometimes encountered in perdeuterated proteins, can be overcome.

Acknowledgements

This work was supported by a grant from the Deutsche Forschungsgemeinschaft (SFB 472) and by a grant from the Fraunhofer-Gesellschaft (E/B31E/M0157/M 5137).

References

Bax, A. and Grzesiek, S. (1993) *Acc. Chem. Res.*, **26**, 131–138.
Bottomley, M.J., Macias, M.J., Liu, Z. and Sattler, M. (1999) *J. Biomol. NMR*, **13**, 381–385.
Cavanagh, J., Palmer III, A.G., Wright, P.E. and Rance, M. (1991) *J. Magn. Reson.*, **91**, 429–436.
Clubb, R.T., Thanabal, V. and Wagner, G. (1992) *J. Magn. Reson.*, **97**, 213–217.
Delaglio, F., Torchia, D.A. and Bax, A. (1991) *J. Biomol. NMR*, **1**, 439–446.
Delaglio, F., Grzesiek, S., Vuister, G.W., Zhu, G., Pfeifer, J. and Bax, A. (1995) *J. Biomol. NMR*, **6**, 277–293.
Dingley, A.J. and Grzesiek, S. (1998) *J. Am. Chem. Soc.*, **120**, 8293–8297.
Emsley, L. and Bodenhausen, G. (1990) *Chem. Phys. Lett.*, **165**, 469–476.
Grzesiek, S. and Bax, A. (1993a) *J. Am. Chem. Soc.*, **115**, 12593–12594.
Grzesiek, S. and Bax, A. (1993b) *J. Biomol. NMR*, **3**, 185–204.
Ikegami, T., Sato, S., Wälchli, M., Kyogoku, Y. and Shirakawa, M. (1997) *J. Magn. Reson.*, **124**, 214–217.
Ikura, M., Kay, L.E. and Bax, A. (1990) *Biochemistry*, **29**, 4659–4667.
Kanelis, V., Donaldson, L., Muhandiram, D.R., Rotin, D., Forman-Kay, J.D. and Kay, L.E. (2000) *J. Biomol. NMR*, **16**, 253–259.
Kay, L.E. and Gardner, K.H. (1997) *Curr. Opin. Struct. Biol.*, **7**, 722–731.
Kay, L.E., Ikura, M., Tschudin, R. and Bax, A. (1990) *J. Magn. Reson.*, **89**, 496–514.
Kay, L.E., Keifer, P. and Saarinen, T. (1992) *J. Am. Chem. Soc.*, **114**, 10663–10665.

Klimmek, O., Stein, T., Pisa, R., Simon, J. and Kröger, A. (1999) *Eur. J. Biochem.*, **263**, 79–84.
Kreis-Kleinschmidt, V., Fahrenholz, F., Kojro, E. and Kröger, A. (1995) *Eur. J. Biochem.*, **227**, 137–142.
Kupče, Ē. and Freeman, R. (1995) *J. Magn. Reson.*, **A115**, 273–276.
Liu, A., Riek, R., Wider, G., von Schroetter, C., Zahn, R. and Wüthrich, K. (2000) *J. Biomol. NMR*, **16**, 127–138.
Logan, T.M., Olejniczak, E.T., Xu, R.X. and Fesik, S.W. (1992) *FEBS Lett.*, **314**, 413–418.
Loria, J.P., Rance, M. and Palmer III, A.G. (1999) *J. Magn. Reson.*, **141**, 180–184.
Marion, D., Ikura, M., Tschudin, R. and Bax, A. (1989) *J. Magn. Reson.*, **85**, 393–399.
Matsuo, H., Kupče, Ē., Li, H. and Wagner, G. (1996) *J. Magn. Reson.*, **B111**, 194–198.
Mattiello, D.L., Warren, W.S., Mueller, L. and Farmer II, B.T. (1996) *J. Am. Chem. Soc.*, **118**, 3253–3261.
Morris, G.A. and Freeman, R. (1979) *J. Am. Chem. Soc.*, **101**, 760–762.
Patt, S. (1992) *J. Magn. Reson.*, **96**, 94–102.
Pervushin, K., Riek, R., Wider, G. and Wüthrich, K. (1997) *Proc. Natl. Acad. Sci. USA*, **94**, 12366–12371.
Pervushin, K., Riek, R., Wider, G. and Wüthrich, K. (1998) *J. Am. Chem. Soc.*, **120**, 6394–6400.
Salzmann, M., Pervushin, K., Wider, G., Senn, H. and Wüthrich, K. (1998) *Proc. Natl. Acad. Sci. USA*, **95**, 13585–13590.
Salzmann, M., Wider, G., Pervushin, K. and Wüthrich, K. (1999a) *J. Biomol. NMR*, **15**, 181–184.
Salzmann, M., Wider, G., Pervushin, K., Senn, H. and Wüthrich, K. (1999b) *J. Am. Chem. Soc.*, **121**, 844–848.
Shaka, A.J., Keeler, J., Frenkiel, T. and Freeman, R. (1983) *J. Magn. Reson.*, **52**, 335–338.
Stonehouse, J., Shaw, G.L., Keeler, J. and Laue, E.D. (1994) *J. Magn. Reson.*, **A107**, 178–184.
Tycko, R., Pines, A. and Guckenheimer, R. (1985) *J. Chem. Phys.*, **83**, 2775–2802.
Wang, A.C., Grzesiek, S., Tschudin, R., Lodi, P.J. and Bax, A. (1995) *J. Biomol. NMR*, **5**, 376–382.
Weisemann, R., Rüterjans, H. and Bermel, W. (1993) *J. Biomol. NMR*, **3**, 113–120.
Wittekind, M. and Mueller, L. (1993) *J. Magn. Reson.*, **B101**, 201–205.
Yang, D. and Kay, L.E. (1999) *J. Biomol. NMR*, **14**, 273–276.